J. Fluid Mech. (2003), *vol.* 482, *pp.* 163–179.
DOI: 10.1017/S0022112003004014 Printed in the United Kingdom

Magnetohydrodynamic damping of convective flows in molten gallium

By B. HOF[1], A. JUEL[2] AND T. MULLIN[1]

[1]Department of Physics and Astronomy, The University of Manchester, Manchester M13 9PL, UK

[2]Department of Mathematics, The University of Manchester, Oxford Road, Manchester M13 9PL, UK
ajuel@maths.man.ac.uk

(Received 8 May 2002 and in revised form 19 July 2002)

We report the results of an experimental study of magnetohydrodynamic damping of sidewall convection in a rectangular enclosure filled with gallium. In particular we investigate the suppression of convection when a steady magnetic field is applied separately in each of the three principal directions of the flow. The strongest damping of the steady flow is found for a vertical magnetic field, which is in agreement with theory. However, we observe that the application of a field transverse to the flow provides greater damping than a longitudinal one, which seems to contradict available theory. We provide a possible resolution of this apparent dichotomy in terms of the length scale of the experiment.

1. Introduction

We present the results of an experimental investigation of buoyancy-driven convection in liquid gallium to which a magnetic field is applied. Such flows arise in crystal growing processes in the semiconductor industry. Our experiment is a laboratory model of the horizontal Bridgman technique which is used in the growth of crystals with a specific form. In general, the homogeneity and quality of single crystals grown from doped semiconductor melts is of interest to the manufacturers of electronic chips (Hurle 1993). In the growth process the temperature gradient between the melt and the solidification front cause convective flows of varying complexity. Oscillatory flows are known to cause unwanted banded layers of dopant concentration, called striations, in the crystal as discovered by Müller & Wiehelm (1964). Hurle (1966) and Utech & Flemings (1966) showed that striations can be eliminated by the application of a DC magnetic field.

Steady convective flows can also cause inhomogeneities in the dopant distribution at a macroscopic level. These are termed axial segregation if they occur along the growth axis and radial segregation if they are in a plane perpendicular to this axis (Garandet & Alboussière 1999). Radial segregation can be suppressed if the crystal is grown under purely diffusive conditions, i.e. in the absence of convective motion as discussed by Garandet & Alboussière (1999). Hence, in order to obtain crystals of very high purity it is desirable to eliminate convection during the growth process.

One way to suppress convection is to grow crystals in micro-gravity and thereby reduce buoyancy effects but this can be prohibitively expensive. An alternative method is to damp the convection by growing the crystals in the presence of a magnetic field (Garandet & Alboussière 1999; Series & Hurle 1991). The convective motion of the electrically conducting melt in a magnetic field generates electrical currents, which

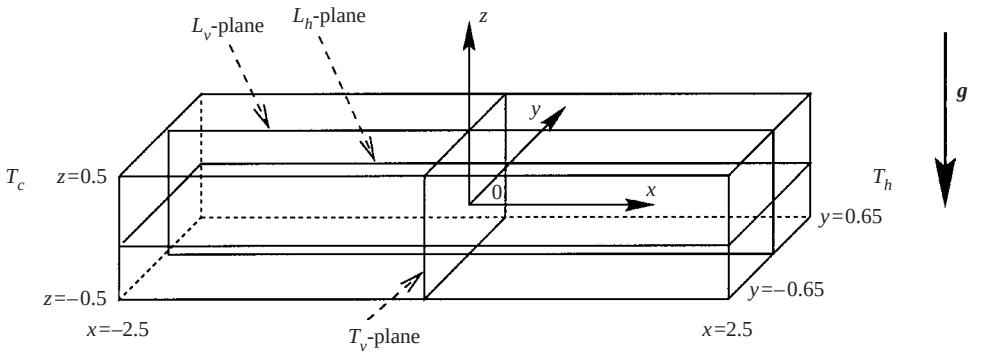

FIGURE 1. Geometry of the system. The T_v, L_v and L_h planes are the central planes orthogonal to the x-, y- and z-directions respectively. T_h (T_c) is the temperature imposed on the right hot (left cold) end-wall.

interact with the magnetic field resulting in a damping force on the flow. The amount of damping will depend on the strength of the applied magnetic field as well as its orientation with respect to the convective circulation.

A schematic diagram of the geometry of our experiment is shown in figure 1. The gallium sample is enclosed in a rectangular cavity of relative dimensions 5.0 : 1.3 : 1.0, and subject to a controlled horizontal temperature difference which drives the convective flow. A steady magnetic field of prescribed strength can be applied in three principal orientations, namely transverse (the magnetic field is orthogonal to the temperature gradient and gravity), vertical (the field is parallel or anti-parallel to gravity) and longitudinal (the field is parallel to the temperature gradient). The control parameters of the flow are the Grashof and Hartmann numbers, Gr and Ha respectively. The former is defined as

$$Gr = \frac{\alpha \Theta g h^4}{l \nu^2},$$

where h (l) is the height (length) of the cavity, ν is the kinematic viscosity, g the gravitational constant, α the coefficient of the thermal expansivity, and $\Theta = T_h - T_c$ the applied temperature difference. Gr measures the relative importance of buoyancy to viscous forces and is proportional to the applied temperature difference. The Hartmann number is defined as

$$Ha = B_0 h \sqrt{\frac{\sigma}{\nu \rho}},$$

where ρ is the density, B_0 the magnetic field and σ the electrical conductivity. Ha is proportional to the strength of the magnetic field and its square is a measure of the relative importance of the electromagnetic to the viscous forces. A further parameter is the Prandtl number $Pr = \nu/\kappa$ which is the ratio of the kinematic viscosity to the thermal diffusivity. For gallium, this parameter is very small, so that most of the heat transport takes place by conduction. Here, the Prandtl number was kept constant at $Pr = 0.019$ by retaining a mean temperature in the gallium sample of approximately 75.0 °C.

Buoyancy-driven convection in the presence of a magnetic field has been the subject of several theoretical and experimental investigations. Garandet & Alboussière (1992) used an analytical approach to investigate the damping effect of a vertical magnetic

field on a two-dimensional convective flow. They found, that in the limit of large Hartmann numbers, the x-component of the velocity, u, is damped in proportion to Ha^{-2}. They extended their theory to cavities of arbitrary cross-section subjected to fields of any orientation (Alboussière, Garandet & Moreau 1996). When applied to rectangular cavities the theory predicts the following scalings for the velocities in the core: a Ha^{-2} scaling of the longitudinal velocity component, u, for a vertical field; a Ha^{-2} scaling of the vertical velocity component, v, for a longitudinal applied field; but only a Ha^{-1} scaling of flow velocities when a transverse field is applied. In the latter orientation strong electrical potentials are created which almost compensate the electromotive force. As a result the damping of convection is weak.

An asymptotic analysis undertaken by Bojarevics (1995) is in accord with the above scaling laws for vertical and transverse fields. In addition, he showed that for a vertical field, the damping in the boundary layers parallel to the magnetic field, the so-called parallel layers, is much weaker than in the core flow, resulting in velocity jets in these layers.

A detailed theoretical study of the three-dimensional flow structure in a rectangular cavity subject to magnetic fields was undertaken by Aleksandrova (2001). The flow structure for high Ha is found to be more uniform in a longitudinal field than in a vertical one, i.e. the velocity jets in the parallel layers are weaker, while both field orientations show the same asymptotic scaling in the core. The heat flux is calculated for cavities of aspect ratio $1:1:1$ and $4:1:1$ for the three principal field orientations. In both aspect ratios the transverse field clearly exhibits the weakest reduction of the heat flux. Whereas, in the cubical cell the longitudinal field damps convection most effectively, in the larger aspect ratio cell, the vertical field shows the strongest reduction of convection.

This latter result is in agreement with the numerical and experimental studies of Ozoe & Okada (1989) and Okada & Ozoe (1992), who investigated the magnetohydrodynamic damping in a cubical cavity. They found that the strongest reduction in heat transfer occurred for a longitudinal field, closely followed by the vertical one. For a transverse field however, the damping was of almost an order of magnitude less.

In three-dimensional numerical calculations for a cell of aspect ratio $4:1:1$ BenHadid & Henry (1997) investigated the damping of the steady flow for vertical and longitudinal magnetic fields. They confirm the core flow velocity scaling laws predicted by the asymptotic theory of Alboussière *et al.* (1996). However in contrast to Okada & Ozoe they find that the vertical field shows a stronger damping of the overall flow than the longitudinal one. The asymptotic Ha^{-2} scaling in the core is reached for the vertical field when $Ha > 20$ whereas in the longitudinal field $Ha > 50$ is required before this regime is achieved. They suggest that the relatively weak damping of the flow in a longitudinal field results from the aspect ratio of the container. The longitudinal field interacts with the z-velocity component and hence the relevant length scale is the height of the container. However, the vertical field acts on the x-velocity component and the relevant length scale is the container length. Since the length is greater than the height for their geometry the application of the vertical field is more effective in damping the flow.

In addition to the longitudinal and vertical field BenHadid & Henry (1994) also consider the damping effect of a transverse magnetic field. They find that the maximum horizontal flow velocity u_{max} in an aspect ratio $4:1:1$ cavity scales as Ha^{-1} for a vertical and longitudinal field. Again the asymptotic scaling sets in at higher Ha for the longitudinal field. No asymptotic scaling law has been found for u_{max} in the

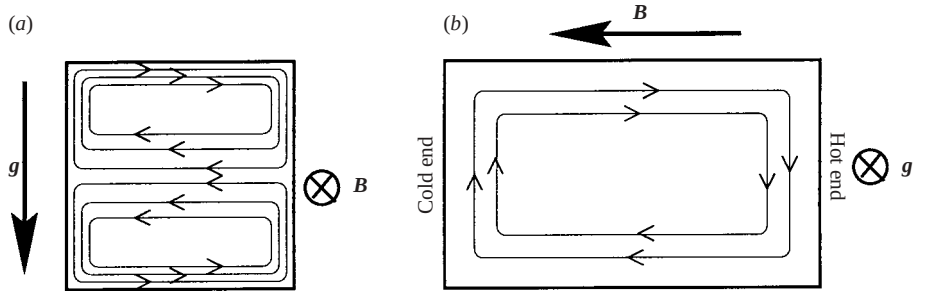

FIGURE 2. Sketches of the current path in a longitudinal magnetic field. (*a*) Currents close in a plane of constant x as suggested by numerical calculations, (*b*) currents close in plane of constant z as suggested by analytical considerations.

transverse field. However the damping of u_{max} is stronger in the transverse than in the longitudinal field.

BenHadid & Henry (1997) also find that in a longitudinal field current paths differ significantly from those expected from analytical models. In these, Garandet & Alboussière (1999) show that currents are expected to close in a plane of constant z, as shown schematically in figure 2(*b*). In BenHadid & Henry's calculations however, currents mainly close in a plane of constant x, as shown schematically in figure 2(*a*). The difference between the numerical and the analytical models discussed above arises because of the aspect ratio. In the $4:1:1$ cell, potential gradients across the cavity are greater than those along the channel.

In contrast to the significant amount of analytical and numerical research discussed above, experimental work remains sparse. Davoust *et al.* (1999) investigate the damping of convection and the reduction in heat transport in a mercury-filled horizontal cylinder, subject to a vertical magnetic field. They find that the axial velocity component scales asymptotically as Ha^{-2} in agreement with the analytical and numerical predictions by Alboussière, Garandet & Moreau (1993) and BenHadid & Henry (1996).

In a combined numerical and experimental study, Juel *et al.* (1999) measure the vertical temperature difference at a given Grashof number for varying Hartmann numbers in a transverse applied field. Experimental and numerical results show excellent agreement and, in particular, flows observed in the calculations become increasingly two-dimensional with increasing Hartmann number.

Despite all the above research it is still not clear which orientation of the magnetic field is the most effective in damping convective flows. Analytical results only apply in the asymptotic regime and are therefore of limited use in practice. Also, because the convective flow is three-dimensional in nature (Juel *et al.* 2001), the limits of applicability of two-dimensional simulations need to be established. Three-dimensional simulations are time consuming and often consider the non-physical case of perfectly conducting fluids ($Pr = 0$) so that heat transfer and flow become uncoupled. Therefore, there is a need for experimental studies in order to clarify which field orientation is the most favourable in practice and to understand how the applied field influences the flow structure.

In the following section we describe the experimental apparatus. In § 3.1 the importance of the control of the thermal boundary conditions is emphasized and the experimental findings are compared with available results from numerical models.

The results of the investigation into the damping of the flow are presented in § 3.2 for transverse, longitudinal and vertical fields. Conclusions are presented in § 4.

2. Experimental apparatus

The experimental apparatus was a development of that described in Braunsfurth & Mullin (1996) and Juel *et al.* (2001), and interested readers are referred there for further details. We have made significant improvements which provide better control of the thermal boundary conditions and allowed us to obtain a good approximation to those applied in numerical models. The central section of the experiment is shown schematically in figure 3. The sample of liquid gallium was held in an insulating enclosure of rectangular cross-section with dimensions 5.0 cm long, 1.3 cm wide and 1.0 cm high resulting in an aspect ratio of 5.0 : 1.3 : 1.0. The sidewalls, top and bottom were 5 mm thick and machined from Lexan, a transparent plastic, of thermal conductivity, $k = 0.2\,\mathrm{W\,m^{-1}\,K^{-1}}$, 150 times smaller than that of gallium. The enclosure had conducting endwalls which were made of 1 mm thick molybdenum sheets. Molybdenum has a thermal conductivity of $k = 142\,\mathrm{W\,m^{-1}\,K^{-1}}$, which is approximately 5 times that of gallium ($k = 30\,\mathrm{W\,m^{-1}\,K^{-1}}$ at 50 °C), and importantly, it is impervious to attack by it.

Gallium oxidizes rapidly if exposed to the atmosphere. In order to avoid the contamination of the initially 99.99% pure sample of gallium, the convection cell was evacuated prior to filling. Two filling nozzles were embedded in the top surface of the enclosure, with one connected via a silicone tube to an o-ring-sealed glass syringe and the other to a vacuum pump. The enclosure was first flooded with helium gas and then evacuated to remove all oxygen from the cell which was then completely filled with gallium and the tube to the vacuum pump was sealed. The connection to the syringe was kept open to allow the gallium to expand into it. This filling procedure also ensured that all walls were fully wetted by gallium.

Each molybdenum endwall was inset into the side of a copper box, through which silicone oil was circulated at a flow rate of $3\,\mathrm{l\,min^{-1}}$. The oil temperature was controlled to within ± 0.01 °C, by commercial circulator baths. Different temperature values were set for each end box, in order to impose the desired horizontal temperature gradient along the sample of gallium.

The experiment was enclosed in a temperature-controlled cabinet. The cabinet temperature was set by a PID controller which heated the air with a 600 W fan heater to a temperature of 35 ± 0.5 °C. Particular care was taken in insulating the convection cell from the ambient temperature. Specifically, the high thermal conductivity of gallium readily facilitates heat loss through the sidewalls of the enclosure. This can significantly alter the steady convective flow as discussed by Juel *et al.* (2001). In order to minimize this effect we followed Davoust *et al.*'s (1999) method and enclosed the convection cell within a copper shield which was in thermal contact with both temperature-controlled end boxes as shown in figure 3. The space between the shield and the enclosure was filled with cotton-wool ($k \simeq 0.04\,\mathrm{W\,m^{-1}\,K^{-1}}$). Hence, a linear temperature gradient was imposed along the length of the enclosure and heat loss through the sidewalls of the enclosure was minimized.

The experiment was mounted onto a 12.5 mm thick aluminium supporting plate, with a 5.0 mm Teflon layer on top to insulate the system both thermally and electrically from the base. As shown in figure 4, the mounting plate could be levelled with respect to the base with three adjustment screws. The whole system was inserted between the iron cores of an electromagnet as shown in figure 4. Magnetic fields of up to 1100 G

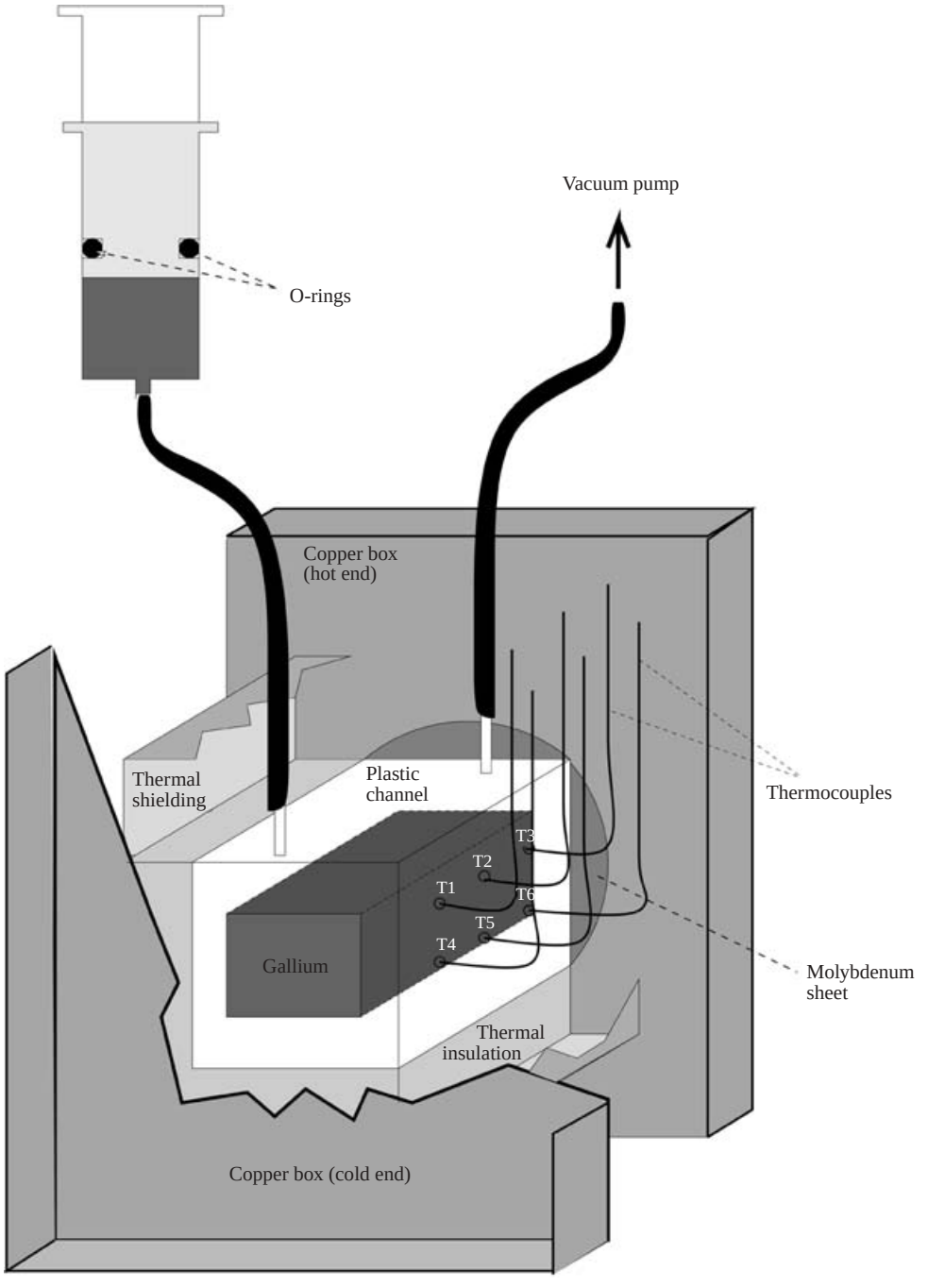

FIGURE 3. Convection cell.

were applied and these were uniform to within 1.5% along the length of the enclosure and 0.5% across its width. The cell could be placed with its endwalls either parallel or perpendicular to the faces of the pole pieces, resulting in longitudinal and transverse orientations of the magnetic fields respectively. In order to apply a vertical magnetic

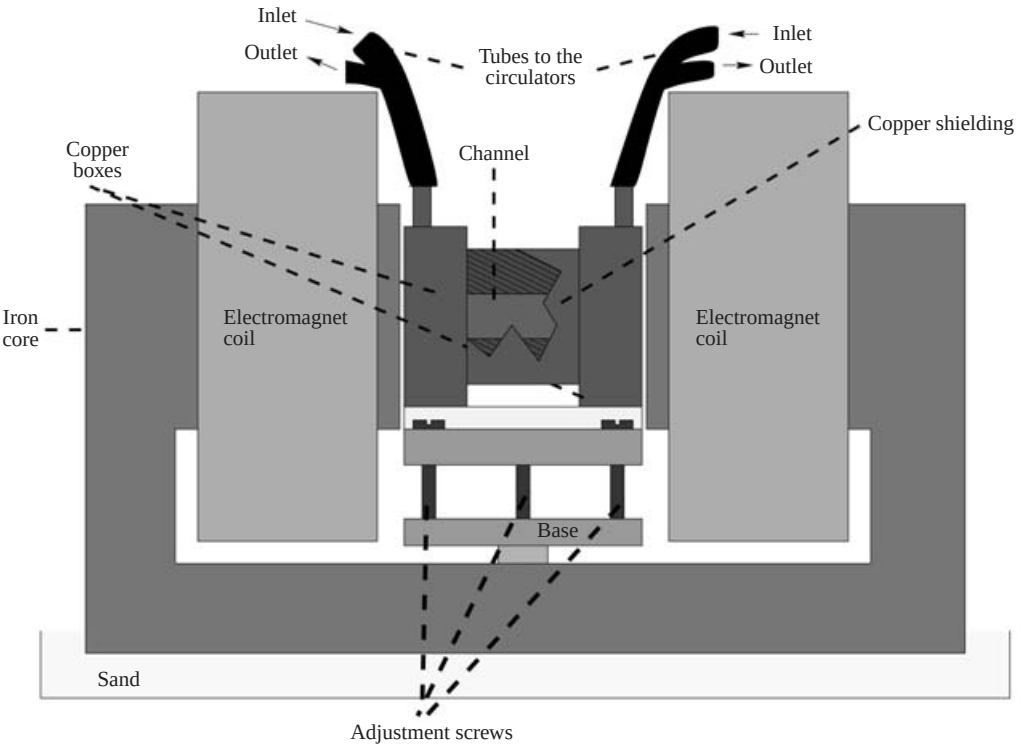

FIGURE 4. Experimental apparatus.

field, the electromagnet was rotated by 90° so that the faces of the pole pieces were oriented perpendicular to gravity. Finally, the entire experiment was placed on a bed of sand, which acted to damp external vibrations.

Measurements of the convective flow were taken with 14 type *K* thermocouple probes of diameter 0.25 mm. They were inserted 1.0 mm into the gallium through 0.4 mm diameter holes in the Lexan enclosure, which were subsequently sealed with epoxy. The cold end junctions of all thermocouples were contained in a temperature-controlled box. The signals were amplified using purpose-built circuitry and sampled onto a PC via a 12 bit A/D board for further processing. All thermocouple probes had been carefully calibrated prior to the measurements. Errors were estimated by the standard deviation of a sampled steady signal and were of order 0.01 K.

The locations at which the probes penetrate the gallium are shown schematically in figure 5. Six probes (T1 to T6) were inserted through the right-hand sidewall (at $y = -0.65$, see figure 5) and six (T7 to T12) through the left-hand sidewall (at $y = +0.65$), at the same locations investigated by Juel (1997). Probes T13 and T14 penetrated the gallium sample at the top surface ($z = 0.5$) on either end of the channel and were used to measure the mean temperature and the temperature difference along the gallium sample. The dependence of the fluid properties of gallium on temperature was discussed by Braunsfurth *et al.* (1997). The data they compiled are used throughout our work to calculate *Pr*, *Ha* and *Gr*.

In preliminary measurements we established that after a change in Grashof number thermal equilibrium was reached in less then 10 minutes (4 longitudinal thermal diffusion times). Hence throughout the experiment we allowed settling times of at

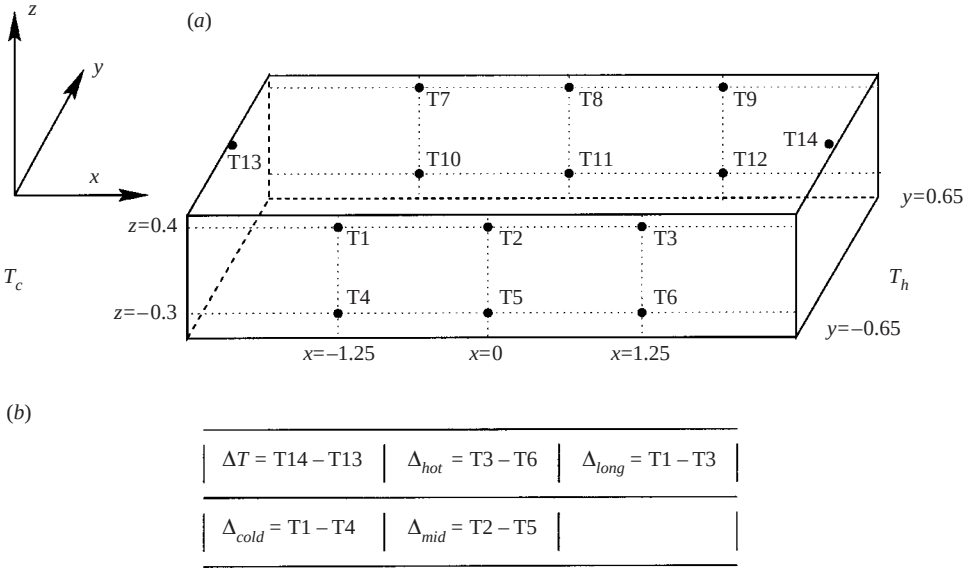

FIGURE 5. (*a*) Positions of the thermocouple probes in the cavity; (*b*) definition of temperature differences, used in the discussion of the results.

least 10 minutes. When data were sampled the settling time was normally extended to 30 minutes to ensure equilibrium conditions.

Vertical and longitudinal temperature differences are used as a measure of the strength of convective flow in the discussion of the results. Vertical temperature differences arise as a direct consequence of convection. If heat is transported by conduction only, e.g. when convection is fully damped by a strong magnetic field, there is a constant temperature gradient along the cavity. Isotherms are then equally spaced in the x-direction and aligned vertically. When the magnetic field is decreased convection increases and the isotherms are bent, signifying vertical temperature differences. Furthermore, the temperature gradient along the cavity is no longer uniform, i.e. the isotherms are no longer equally spaced. The convective contribution to the heat transport is strongest in the central part of the cavity, causing longitudinal temperature gradients in the core to decrease, i.e. the spacing of the isotherms to increase. Since the horizontal heat flux is constant throughout the cavity horizontal temperature gradients increase close to the hot and cold endwalls where the convective heat transport is small. As a consequence of this, a longitudinal temperature difference measured between two points in the cavity (e.g. T1–T3 in figure 5*a*) at a given Grashof number will vary with *Ha*.

3. Results

The experimental methods outlined above were used to investigate properties of steady flows both with and without an applied magnetic field. The initial results, presented in § 3.1 were used to investigate the symmetry properties of the flow from the temperature distribution in the convective flow. Once this was established, a magnetic field was applied in three different directions and its effect on convection was studied. The results of this study are presented in § 3.2.

3.1. *Symmetry of the steady flow*

Steady convective flows calculated for thermally insulating rectangular enclosures (e.g. BenHadid & Henry 1997) are symmetric to rotations of π about the y-axis (rotation-symmetry) and to reflections with respect to the L_v plane (left–right symmetry). However, in the experimental flows of Hurle, Jakeman & Johnson (1974), Braunsfurth *et al.* (1997) and Juel *et al.* (1999) this rotation-symmetry is not usually observed. As in any physical system, imperfections tend to break the perfect symmetries assumed in models. For example Juel *et al.* (1999) and Juel *et al.* (2001) report that symmetry aspects of the flow sensitively depend on the ambient temperature. Whereas in numerical calculations Juel *et al.* (1999) find that the maximum vertical temperature difference is situated halfway between the hot and the cold endwall, in the experiment they find that the maximum vertical temperature difference is shifted from the central plane which corresponds to the T_v-plane in figure 1. Moreover, Juel *et al.* observe that the magnitude and direction of the displacement depends on the ambient temperature. This suggests that the loss of the rotation-symmetry in the experiments may be a result of heat losses through the imperfect insulation of the container. The first goal of the experiment was therefore to test the symmetry of the flow.

In this section, we show that a close approximation to an rotation-symmetric steady flow is obtained when the convection cell is thermally shielded as described in § 2. The influence of the heat shield on the symmetry properties of the steady flow was established in successive experiments which were carried out with and without the shield. The same experimental procedure was applied in both cases: On each run of the experiment two vertical temperature differences were recorded for Grashof numbers between 0 and 3.7×10^4. One temperature difference was measured halfway between the T_v plane and the hot endwall, Δ_{hot} (see figure 5*b*), the second halfway between the T_v plane and the cold endwall, Δ_{cold}. Gr was increased from zero in steps of 600 and the flow was left to settle for 30 minutes between temperature increments. Data were then sampled for 15 minutes at a frequency of 1 Hz.

The difference $\Delta_{diff} = \Delta_{hot} - \Delta_{cold}$ was used as a measure of the symmetry of the steady flow. Note that the probe positions T1 and T4 do not exactly map onto T3 and T6 when rotated by 180° about the y-axis (see figure 5) The rotation results in a small shift of $\Delta z = -1$ mm of the probe positions. Hence there is a small difference in the magnitude of Δ_{hot} and Δ_{cold} for large Gr even in a perfectly symmetric flow, but calculations performed by Juel (1997) show that this difference is less than 3%. Hence for a symmetric flow Δ_{hot} and Δ_{cold} will be equal to within the experimental error of 0.01 K even at high Gr, and Δ_{diff} is therefore a suitable measure of the rotation-symmetry of the flow.

The measurements of Δ_{diff} for the shielded and unshielded experiment are compared in figure 6(*a*). All measurements were made for Grashof numbers below the onset of time dependence. It can be seen that in the unshielded cavity Δ_{diff} increased monotonically with increasing Gr to values greater than 0.4 K when $\Delta_{cold} = 0.7$ K. However Δ_{diff} remains an order of magnitude smaller over the Grashof number range investigated for the case of the shielded cell.

In order to quantify the magnitude of the loss of the rotation-symmetry at a given Gr we introduce the relative asymmetry defined as $\Delta_{rel} = (\Delta_{hot} - \Delta_{cold})/(\Delta_{hot} + \Delta_{cold})$. This quantity varies between ± 1. It is zero for a perfectly symmetric flow and $+1$ (-1) if convection is localized close to the hot (cold) wall and the heat transport is mainly conductive in the rest of the enclosure.

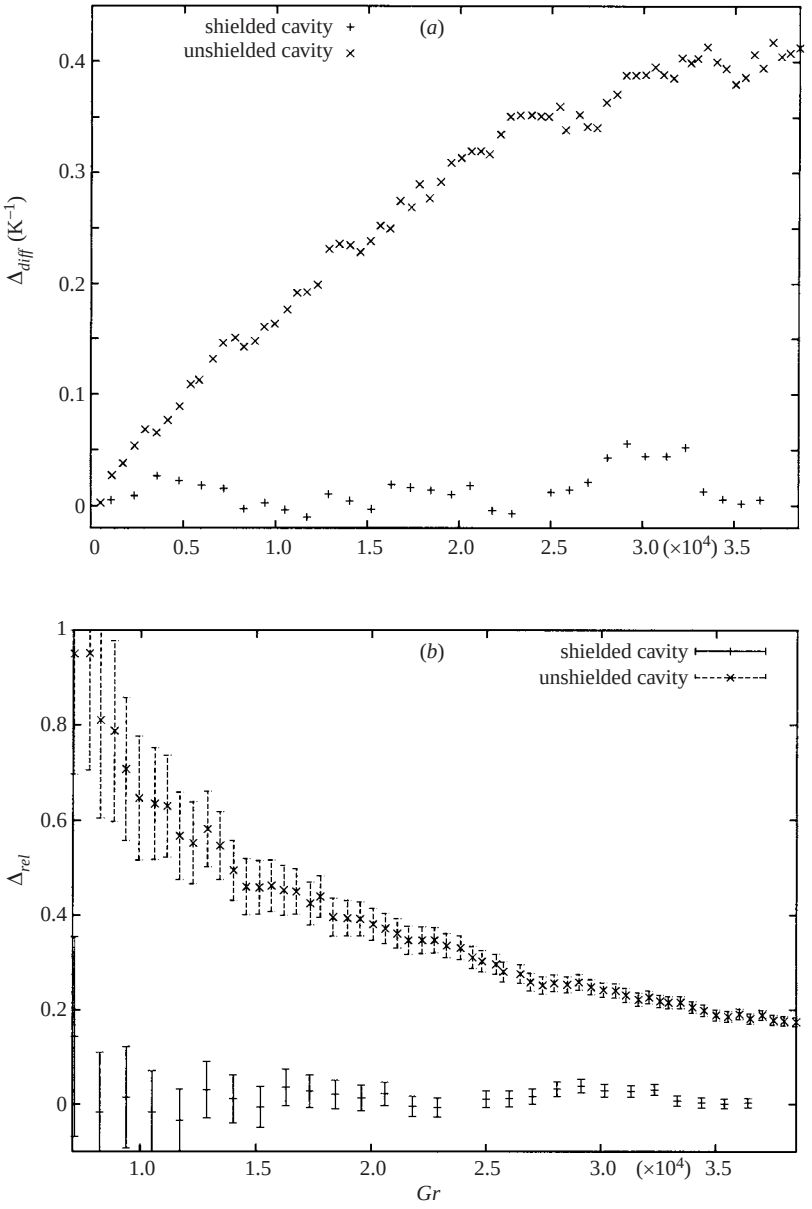

FIGURE 6. (*a*) Difference between two vertical temperature differences measured symmetrically about the T_v plane plotted as a function of *Gr*. (*b*) Relative asymmetry of the flow as a function of *Gr*, see text for details.

The relative asymmetry is plotted as a function of Grashof number in figure 6(*b*). Data points for $Gr < 7 \times 10^3$ are omitted because for these values the signal-to-noise ratio is smaller than 1. For the unshielded cavity the relative asymmetry is close to 1 for small Grashof numbers and convection is localized towards the hot endwall. The value of the relative asymmetry then decreases with increasing Grashof number. The distortion of the convection roll varies significantly with Grashof number, which suggests that the flow is influenced by uncontrolled heat losses to the environment.

In the shielded cavity the relative asymmetry is approximately zero within the experimental errors over the entire range of *Gr*. Thus the convective flow is independent of the ambient temperature and closely symmetric to a rotation of 180° about the *y*-axis. Measurements taken from the thermocouple probes close to the opposite sidewall (T7 to T12) support this result, and also show that the flow is to a good approximation left–right symmetric. Hence, in the shielded system, the steady flow exhibits close agreement with the symmetry properties of the flow in the numerical models (BenHadid & Henry 1997).

3.2. *Magnetohydrodynamic damping of the steady flow*

The main objective of this part of the investigation was to establish which of the three orientations of the applied magnetic field was the most effective in damping steady convective flows. Temperature differences were measured over a range of Hartmann numbers for each of the three orientations of the magnetic field and thereby the effect of the field on convection was monitored. In each experiment the Grashof number was increased from zero quasi-statically, i.e. *Gr* was incremented in steps of 250 with settling times of 10 minutes between increments up to values between 3.7×10^4 and 3.9×10^4, which were just below the onset of time dependence. For the vertical and longitudinal field *Gr* was set to 3.75×10^4 whereas a slightly higher value of $Gr = 3.9 \times 10^4$ was used for the transverse field. Once this Grashof number was established it was kept constant and the magnetic field was increased in steps of $\Delta Ha = 2.5$ starting from zero. Between increments, the flow was left to settle for 30 minutes and temperatures were monitored for a further 30 minutes at a sampling rate of 5 Hz. This procedure was continued until a maximum Hartmann number of 50 was reached.

The vertical temperature difference $\overline{\Delta_{mid}} = (\Delta_{mid}(Ha)/\Delta_{mid}(Ha = 0))$ is shown in figure 7 for vertical, transverse and longitudinal field orientations. As discussed in § 2 vertical temperature differences give a measure of the heat transport by convection. Furthermore it should be noted that the variation of Δ_{mid} was qualitatively the same as that found at all other measuring stations. Hence vertical temperature differences throughout the cavity showed the same scaling with *Ha*.

The strongest variation of Δ_{mid} with Hartmann number is found for the vertical field as may be clearly seen in figure 7. Here Δ_{mid} decreases monotonically for all Hartmann numbers. At approximately $Ha = 8$ the curve has an inflection point and starts to asymptote towards a zero temperature difference. From $Ha \geqslant 40$ the vertical temperature differences measured are zero within the experimental error. This suggests that isotherms are parallel to the endwalls so that the heat transport is almost purely conductive and therefore convection is strongly damped. In figure 8(*a*) the data set for a vertical field is plotted on a log–log scale together with the vertical temperature differences calculated from the analytical solution (Garandet & Alboussière 1992, equation (10)) for the two-dimensional core flow in a rectangular cavity with isothermal boundaries, subject to a vertical magnetic field. The latter is the difference between the temperatures at positions $z = 0.4$ and $z = -0.3$ for $Gr = 37500$ and $Pr = 0.019$ and it is normalized by the zero *Ha* value. Whereas the calculated vertical temperature difference in the asymptotic regime decays in proportion to Ha^{-2}, the experimental data shows a decay rate of $Ha^{-3.5}$ for $25 < Ha < 40$. Indeed a ln–linear plot of the data as shown in figure 8(*b*) suggests that Δ_{mid} scales exponentially with Hartmann number. Hence the damping of the vertical temperature differences is significantly stronger than the Ha^{-2} scaling predicted by the theoretical models.

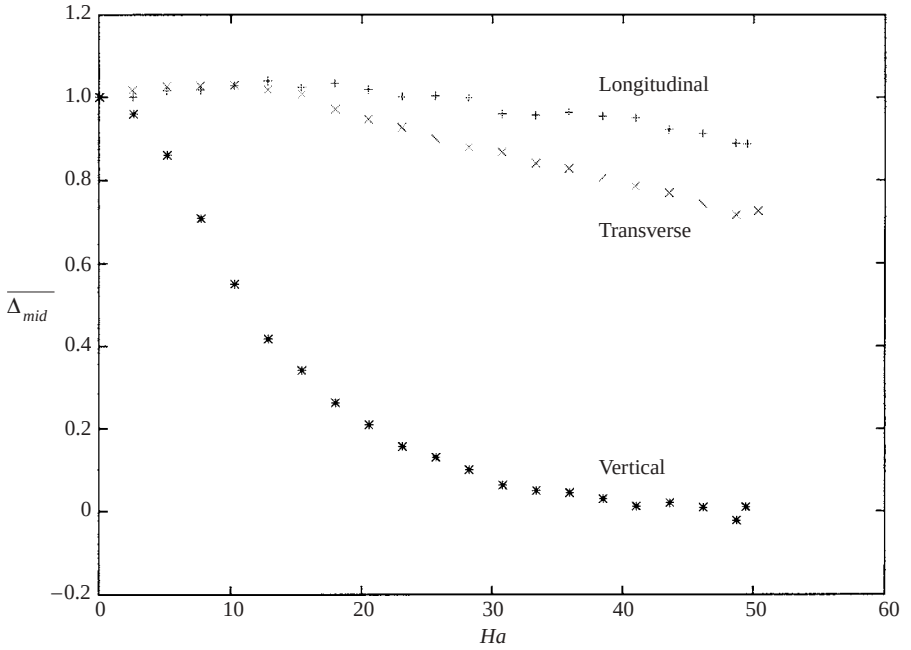

FIGURE 7. The variation of the vertical temperature difference with Hartmann number: ✳, vertical field ($Gr = 3.75 \times 10^4$); ×, transverse field ($Gr = 3.9 \times 10^4$); +, longitudinal field ($Gr = 3.75 \times 10^4$).

For the transverse field the decrease in the temperature difference with increase of Ha is more moderate than for the vertical field. For small Hartmann numbers ($Ha < 10$) the temperature difference displays a small increase over the zero field value. From $Ha > 10$, Δ_{mid} decays at a more or less even rate up to a value of 0.725 at $Ha = 50$. In their study, Juel *et al.* (1999) measured a vertical temperature gradient in the centre of an aspect ratio 4 : 1 : 1 cavity and found excellent agreement with three-dimensional numerical calculations. A log–log plot of the transverse field data of the present study together with a reproduction of the data of Juel *et al.* is shown in figure 9. All three data sets are normalized. For $Ha > 25$ the agreement between the sets of data is excellent. This suggests that at large Hartmann numbers vertical temperature differences measured close to the sidewalls show the same scaling as those measured in the centre of the enclosure. At small Hartmann numbers however the measured vertical temperature differences show an increase, which is possibly caused by an enhancement of convection. Neither the numerical nor the experimental data of Juel *et al.* show this increase in the vertical temperature difference over the zero Hartmann number value. Davoust *et al.* (1999) however observed a similar enhancement of the temperature differences measured on the lateral boundaries of their cylinder in the presence of small magnetic fields.

The effect of a longitudinal field is very similar to that of a transverse one. Again for a small magnetic field ($Ha < 20$), the temperature difference increases slightly and then starts to decay with increasing Ha. The decrease of the temperature difference is less than for the vertical and the transverse fields and the lowest relative temperature difference reached is $\overline{\Delta_{mid}} = 0.888$ at $Ha = 50$. Thus the transverse field reduces the

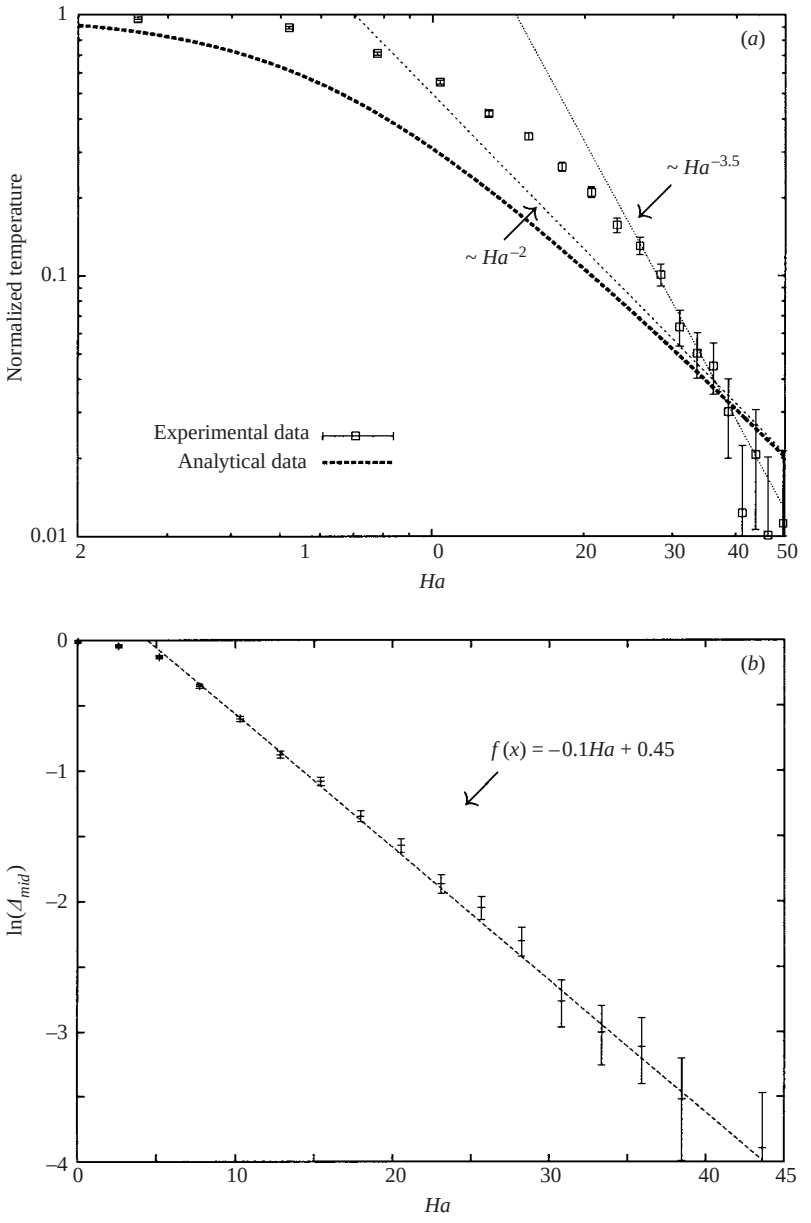

FIGURE 8. (*a*) Log–log plot of the experimental data for $\overline{\Delta_{mid}}$ in the vertical magnetic field (⊡) and data calculated based on the analytical solution for the fully developed flow (Garandet & Alboussière 1992). (*b*) Natural logarithm of the vertical temperature difference $\overline{\Delta_{mid}}$ plotted as a function of Hartmann number in a vertical magnetic field. For $Ha > 35$ the signal-to-noise ratio is smaller than 1, which results in an increased scatter in the data points.

vertical temperature difference by 28% and the longitudinal field by 11% whereas it vanishes in the vertical field.

The longitudinal temperature difference $\Delta_{long} = \mathrm{T3} - \mathrm{T1}$ is shown in figure 10, again plotted as a function of *Ha*. The data are displayed in a normalized form $\overline{\Delta_{long}} = \Delta_{long}(Ha)/\Delta_{long}(Ha = 0)$ for the three field orientations. As expected $\overline{\Delta_{long}}$

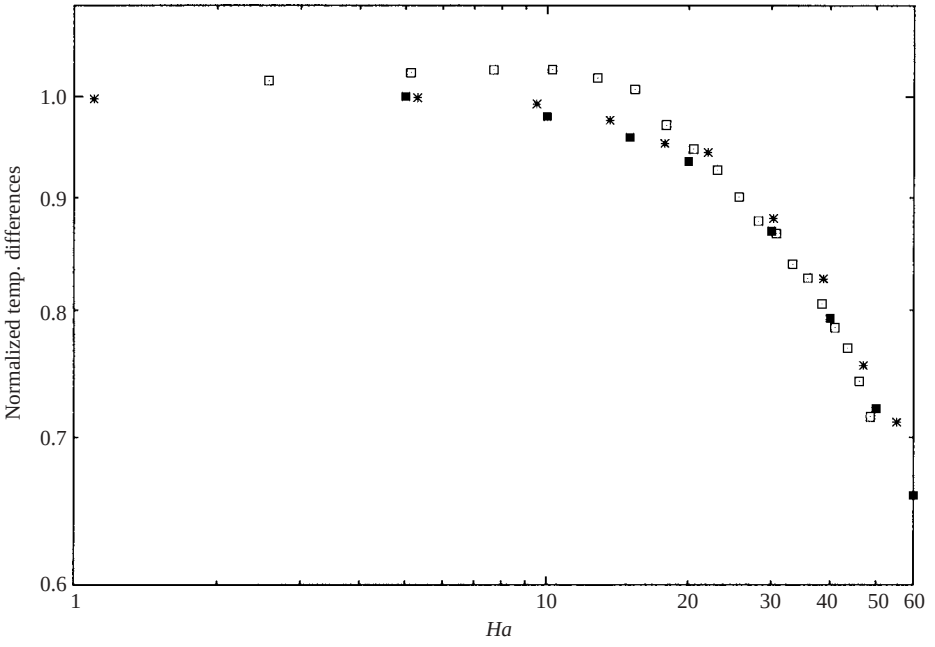

FIGURE 9. Comparison of the data of Juel *et al.* (1999) (■, numerical data; ✳, experimental data) to the experimental data of the present study (⊡). All data sets are normalized.

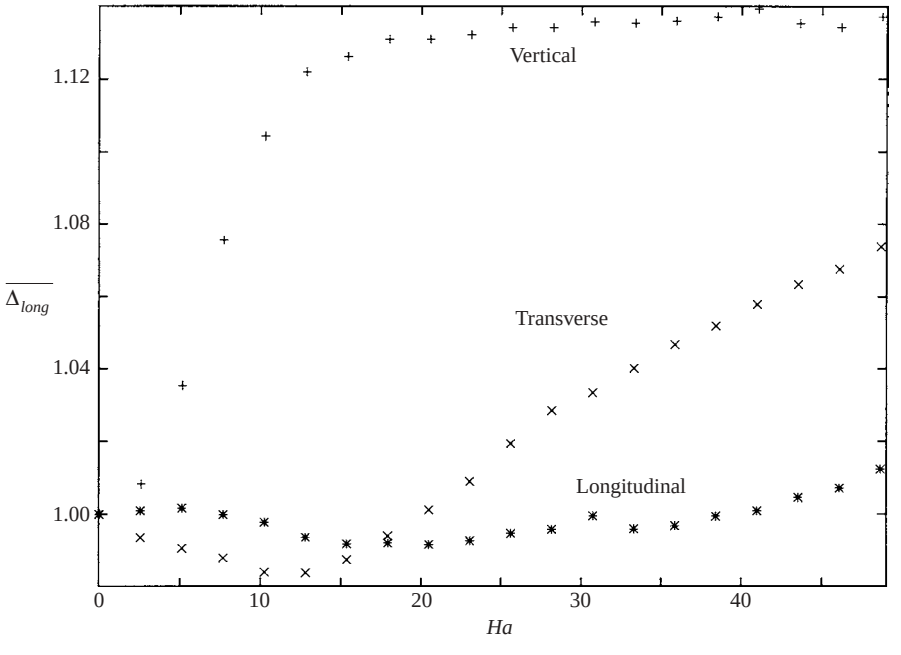

FIGURE 10. The variation of the longitudinal temperature difference $\overline{\Delta_{long}}$ with Hartmann number: +, vertical field; ✳, longitudinal field; ×, transverse field.

increases with increasing Hartmann number towards its conductive value. Consistent with the results shown in figure 7, the vertical field has the strongest effect. Here the asymptotic value reached in the high Hartmann number limit is 14% higher than the value of Δ_{long} at $Ha = 0$. It is interesting to note that in figure 10 the asymptotic value is approached more swiftly than in figure 7. For example, at $Ha = 18$, $\overline{\Delta_{long}}$ has reached 95% of its final value, whereas $\overline{\Delta_{mid}}$ has only decayed by 74%. Similarly in the transverse field case, the asymptotic value is approached more closely for $\overline{\Delta_{long}}$ than for $\overline{\Delta_{mid}}$. Whereas for $Ha = 50$, $\overline{\Delta_{mid}}$ is reduced by 28%, $\overline{\Delta_{long}}$ has increased by 54% of the total increase of $\overline{\Delta_{long}}$. For the longitudinal field however $\overline{\Delta_{long}}$ has only increased by 9% of the total increase at $Ha = 50$, which is slightly less than the decrease of 11% of $\overline{\Delta_{mid}}$ at the same Hartmann number. Hence in the vertical and the transverse fields, longitudinal temperature differences approach the asymptotic value more rapidly than vertical temperature differences. This is not the case in the longitudinal field, which suggests that the flow structure here is different to that in a vertical or transverse field.

As pointed out in the introduction, the container height is the relevant length scale for the strength of the Joule dissipation in a longitudinal field. This at least partially explains why the damping of steady convection in cells of length-to-height ratio greater than unity is comparatively weak in a longitudinal magnetic field. The aspect ratio is also important in the scaling of the top and bottom parallel layers in a longitudinal magnetic field. The thickness of these layers scales in proportion to $\sqrt{1/Ha}\sqrt{l/h}$ whereas the thickness of the parallel layers in a vertical field is independent of the aspect ratio. Hence in a large-aspect-ratio cavity with an applied longitudinal field higher Hartmann numbers are necessary until the asymptotic regime and the strong core flow damping is established.

The length-to-width ratio is also important in determining the current paths in the cavity as discussed in the introduction. The current paths calculated by BenHadid & Henry (1994) for an aspect ratio $4:1:1$ ($l/w = 4$) cell are shown schematically in figure 2(*a*). Here the current loops are mainly contained in planes of constant x and close in the parallel layers at the top and bottom of the cross-section. The magnetic field is perpendicular to the currents in these parallel layers, and it exhibits an accelerating force which hence counteracts the damping in the central part of the cross-section. However in cells of length-to-width ratio smaller than unity, the currents are expected to close in lengthwise horizontal loops, as shown in figure 2(*b*). Currents along the two sidewalls are parallel to the longitudinal field and hence do not give rise to an accelerating Lorentz force. Therefore the damping of the longitudinal field ought to be more efficient in cubic cells than in channels of length-to-width ratio greater than unity.

4. Conclusion

We have shown that the convective steady flow in the experiment is a good approximation of that in numerical models. However to achieve this almost symmetric flow special care had to be taken in the control of the thermal boundary conditions. Since the rotation-symmetry of the flow is sensitively dependent on the thermal boundary conditions, it is unlikely that flows in Bridgman crystal growth facilities will contain this symmetry. This suggests that in order to model convective flows in crystal growth applications, heat losses need to be taken into account. It is interesting to note that the temperature amplitudes shown in figure 9 show the same scaling for

symmetric and non-symmetric flows. Hence breaking the rotation-symmetry does not appear to affect this scaling, which is therefore a robust feature.

The strong damping of steady convection in a vertical magnetic field observed here is qualitative in agreement with analytical (Garandet & Alboussière 1999) and numerical predictions (BenHadid & Henry 1994). However the decay rate found in the experiment is exponential and hence much stronger than the Ha^{-2} scaling expected from analytical considerations. As expected from the numerical work by BenHadid & Henry (1997) the suppression of convection by a longitudinal field is somewhat weaker than for a vertical field because of the aspect ratio.

Perhaps the most surprising result of this study is that in our experiment the transverse field shows a stronger damping effect than the longitudinal one. As discussed in the introduction, analytical considerations suggest that in the transverse field configuration large electrical potentials are created which almost compensate the electromotive force, resulting in a weaker damping than for the vertical and longitudinal field configurations.

We speculate that the asymptotic regime in the longitudinal field is delayed to higher Hartmann numbers because the length-to-height ratio is greater than unity and because the changes in current path give rise to accelerating Lorentz forces in the parallel layers.

We thank the referees for their helpful comments which clarified several issues associated with this work.

REFERENCES

Alboussière, T., Garandet, J. & Moreau, R. 1993 Buoyancy-driven convection with a uniform magnetic field. Part 1. Asymptotic analysis. *J. Fluid Mech.* **253**, 545–563.

Alboussière, T., Garandet, J. & Moreau, R. 1996 Asymptotic analysis and symmetry in mhd convection. *Phys. Fluids* **8**, 2215–2226.

Aleksandrova, S. 2001 Buoyant convection in cavities in a strong magnetic field. PhD thesis, Coventry University.

BenHadid, H. & Henry, D. 1994 Numerical simulations of convective three-dimensional flows in a horizontal bridgman configuration under the action of a constant magnetic field. In *Proc. Second Intl Conf on Energy Transfer in Magneto-Hydrodynamic Flows*, vol. 1, pp. 47–56. Pamir Publications.

BenHadid, H. & Henry, D. 1996 Numerical simulations of convective three-dimensional flows in a horizontal cylinder under the action of a constant magnetic field. *J. Cryst. Growth* **166**, 436–445.

BenHadid, H. & Henry, D. 1997 Numerical study of convection in the horizontal bridgman configuration under the action of a constant magnetic field. Part 2. Three-dimensional flow. *J. Fluid Mech* **333**, 57–83.

Bojarevics, V. 1995 Buoyancy driven flow and its stability in a horizontal rectangular channel with an arbitrary oriented transversal magnetic field. *Magnetohydrodynamics* **31**, 245–253.

Braunsfurth, M. & Mullin, T. 1996 An experimental study of oscillatory convection in liquid gallium. *J. Fluid Mech.* **327**, 199–219.

Braunsfurth, M., Skeldon, A., Juel, A., Mullin, T. & Riley, D. 1997 Free convection in liquid gallium. *J. Fluid Mech.* **342**, 295–314.

Davoust, L., Cowley, M., Moreau, R. & Bolcato, R. 1999 Buoyancy-driven convection with a uniform magnetic field. Part 2. Experimental investigation. *J. Fluid Mech.* **400**, 59–90.

Garandet, J. & Alboussière, T. 1992 Buoyancy driven convection in a rectangular enclosure with a transverse magnetic field. *Intl J. Heat Mass Transfer* **35**, 741–748.

Garandet, J. & Alboussière, T. 1999 Bridgman growth: modelling and experiments. *Prog. Cryst. Growth* **38**, 73–132.

Hurle, D. 1966 Temperature oscillations in molten metals and their relationship to growth striae in melt-grown crystals. *Phil. Mag.* **13**, 305–310.

Hurle, D. T. J. 1993 *Crystal Growing from the Melt*. Springer.

Hurle, D., Jakeman, E. & Johnson, C. 1974 Convective temperature oscillations in molten gallium. *J. Fluid Mech.* **64**, 565–576.

Juel, A. 1997 Magnetohydrodynamic convection in molten gallium. PhD thesis, University of Oxford.

Juel, A., Mullin, T., BenHadid, H. & Henry, D. 1999 Magnetohydrodynamic convection in molten gallium. *J. Fluid Mech.* **378**, 97–118.

Juel, A., Mullin, T., BenHadid, H. & Henry, D. 2001 Three-dimensional free convection in molten gallium. *J. Fluid Mech.* **436**, 267–281.

Müller, A. & Wiehelm, M. 1964 Periodische temperaturschwankungen in fluessigem insb als ursache schichtweisen einbaus von te in kristallisierendes insb. *Z. Naturf.* A **19**, 254–263.

Okada, K. & Ozoe, H. 1992 Experimental heat transfer rates of natural convection of molten gallium suppressed under an external magnetic field in either x, y or z direction. *J. Heat Transfer* **114**, 107–114.

Ozoe, H. & Okada, K. 1989 The effect of the direction of the external magnetic field on the three-dimensional natural convection in a cubical enclosure. *Intl J. Heat Mass Transfer* **32**, 1939–1954.

Series, R. & Hurle, D. 1991 The use of magnetic fields in semiconductor crystal growth. *J. Cryst. Growth* **113**, 305–328.

Utech, H. & Flemings, M. 1966 Elimination of solute banding in indium antimonide crystals by growth in a magnetic field. *J. Appl. Phys.* **37**, 2021–2024.